Journal of Anatomy

J. Anat. (2008) **213**, pp79–85 doi: 10.1111/j.1469-7580.2008.00918.x

Alterations in renal cilium length during transient complete ureteral obstruction in the mouse

Leanne Wang, Raphael Weidenfeld, Elizabeth Verghese, Sharon D. Ricardo and James A. Deane

Monash Immunology and Stem Cell Laboratories, Monash University, Australia

Abstract

The renal cilium is a non-motile sensory organelle that has been implicated in the control of epithelial phenotype in the kidney. The contribution of renal cilium defects to cystic kidney disease has been the subject of intense study. However, very little is known of the behaviour of this organelle during renal injury and repair. Here we investigate the distribution and dimensions of renal cilia in a mouse model of unilateral ureteral obstruction and reversal of ureteral obstruction. An approximate doubling in the length of renal cilia was observed throughout the nephron and collecting duct of the kidney after 10 days of unilateral ureteral obstruction. A normalization of cilium length was observed during the resolution of renal injury that occurs following the release of ureteral obstruction. Thus variations in the length of the renal cilium appear to be a previously unappreciated indicator of the status of renal injury and repair. Furthermore, increased cilium length following renal injury has implications for the specification of epithelial phenotype during repair of the renal tubule and duct.

Key words Bowman's capsule; collecting duct; epithelial; renal cilium; renal tubule; unilateral ureteral obstruction.

Introduction

Primary cilia are non-motile, microtubule-based organelles that extend from the cell surface and are found in many tissues throughout the vertebrate body (Wheatley et al. 1996). The vertebrate kidney is a complex system of tubules and ducts lined by epithelial cells which, with the exception of intercalated cells, bear a primary cilium (Bulger et al. 1974; Webber & Lee, 1974, 1975). Primary cilia in the kidney have recently become the subject of intense investigation since it was discovered that defects of this organelle cause polycystic kidney disease (Pazour et al. 2000; Yoder et al. 2002). Polycystic kidney disease is a common inherited disorder characterized by the formation of fluid-filled cysts throughout the kidney and an associated reduction of renal function (Wilson, 2004). The pathogenesis of polycystic kidney disease involves a loss of epithelial differentiation and inappropriate cell proliferation that has been linked to the role of the renal cilium as a flow sensor (Praetorius et al. 2003; Praetorius & Spring, 2003a,b). *In vitro* studies have demonstrated that deflection of the renal cilium results in a polycystin-1- and polycystin-2-mediated increase in cytoplasmic calcium levels that appears to be necessary for the maintenance of epithelial phenotype in the renal tubule and duct (Nauli et al. 2003). The major factor influencing the susceptibility of the cilium to flow-induced deflection appears to be its length (Schwartz et al. 1997; Resnick & Hopfer, 2007). Several other signalling pathways that influence epithelial phenotype and have been implicated in PKD or related conditions, also have components that localize to the renal cilium (Yoder et al. 2006).

Although the role of the renal cilium in the maintenance of renal architecture has been well studied, less is known about the behaviour of this organelle during epithelial injury and repair. Acute injury of the renal tubule frequently results in epithelial cells acquiring a dedifferentiated/mesenchymal phenotype, a process that can contribute to irreversible fibrotic injury (Liu, 2004). The re-establishment of a differentiated and functional epithelial layer is an important part of repair after acute tubular injury (Bonventre, 2003) and is potentially influenced by cilium-mediated signalling. A study of mouse models of renal injury has established that renal injury results in changes in the length of renal cilia that may alter their sensory capacity and impact on epithelial phenotype (Verghese et al. 2008). Here we use the mouse model of unilateral ureteral obstruction (UUO) and reversal of ureteral obstruction (R-UUO) to further explore the distribution and length of renal cilia during tubular injury and repair. UUO is a reversible condition induced by mechanically preventing urine flow through the ureter and results in damage to the nephron, the basic

Correspondence
Dr James A. Deane, Monash Medical Centre, Level 5/Block E246, Clayton Rd, Clayton, Victoria 3168, Australia.
T: +61 3 95945525; F: +61 3 95946495;
E: james.deane@med.monash.edu.au

Accepted for publication *16 April 2008*
Article published online *5 June 2008*

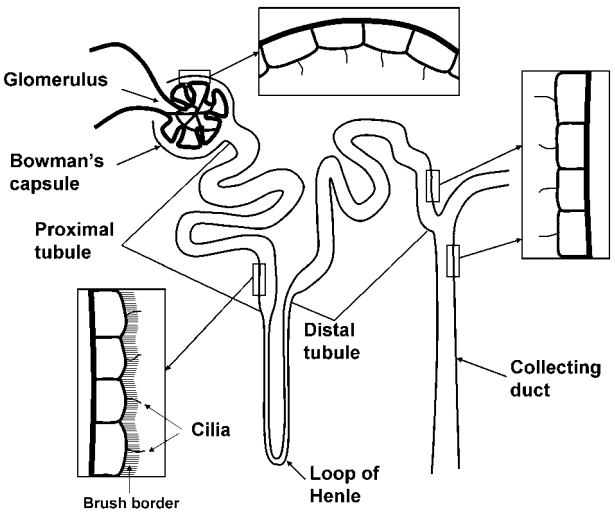

Fig. 1 A diagram of the nephron and collecting duct system depicting the arrangement of renal cilia in segments studied (not to scale). The nephron is composed of the glomerulus including Bowman's capsule, the proximal tubule with a brush border, the loop of Henle, and the distal tubule. Urine production is initiated in the glomerulus and flows through the nephron into the collecting duct.

functional unit of the kidney, and the collecting duct system to which it is attached. The nephron and collecting duct, and the arrangement of renal cilia investigated are depicted in Fig. 1.

Methods

Induction and reversal of unilateral ureteral obstruction injury

Experimentation with animals was approved in advance by the Monash University Animal Ethics Committee, and carried out in adherence to the 'Australian Code of Practice for the Care and Use of Animals for Scientific Purposes'. To induce UUO injury, male C57bl/6J mice (6–8 weeks, 20–25 g) were anaesthetized with 2% inhaled isofluorane (Abbott Australasia, Kurnell, Australia). A small left flank incision was made to access the kidney and the ureter was obstructed using a stainless steel B-1V vascular clamp (0.4–1.0 mm; S & T Fine Science Tools, Foster City, CA, USA). Incisions were sutured and the ureter remained obstructed for 10 days before kidney collection for analysis of obstruction injury, or a second surgery to reverse obstruction and initiate repair. Surgery for R-UUO was as for the induction of UUO with the exception that the vascular clamp was carefully removed from the ureter to allow urine reflow. Successful reversal of obstruction was verified by the appearance of the kidney at collection and by subsequent histological analysis. Three mice were used for each time point investigated.

Histology and immunohistochemistry

Mice used for histology and immunohistochemistry were deeply anaesthetized with isofluorane and perfusion fixed via the left ventricle with 4% paraformaldehyde in phosphate-buffered saline. Kidneys were removed, embedded in paraffin, sectioned and haematoxylin and eosin stained to assess the extent of renal injury. Immunofluorescence staining used boiling citrate buffer (10 mM sodium citrate) for antigen retrieval and the M.O.M™ Immunodetection kit (Vector Laboratories, Burlingame, CA, USA) to allow the use of mouse primary antibodies and block non-specific antibody binding. Primary antibodies against acetylated α-tubulin (Sigma, St. Louis, MO, USA) and aquaporin-1 (Chemicon, Temecula, CA, USA) were visualized with anti-mouse Alexa Fluor 488 and anti-rabbit Alexa Fluor 555 (all from Molecular Probes, Eugene, OR, USA) secondary antibodies, respectively. Primary antibodies were used at a 1 : 500 dilution and secondary antibodies at 1 : 1000. Cell nuclei were stained with DAPI (Molecular Probes, Mt Waverley, VIC, Australia). Specimens were mounted in DAKO fluorescence mounting media (DAKO Cytomation, Botany, NSW, Australia) and viewed using an Olympus Provis AX70 (Olympus, Tokyo, Japan) fluorescence microscope at Monash Micro-Imaging.

Cilium length quantification

Images of randomly selected cilia oriented parallel to the plane of focus were captured in the kidney cortex and medulla using the F-view black and white camera (Olympus) and a high-power oil-immersion objective lens (×100 objective). Images were captured if the full extent of a cilium could be visualized in a single plane of focus. Aquaporin-1 staining was used to visualize the proximal tubule brush border and distinguish the proximal tubule from the distal tubule and collecting duct. Twenty proximal tubules, 20 distal tubule/collecting ducts and 20 parietal epithelial cilia were captured for each mouse. Images of cilia were traced and measured with additional digital zoom (×200) using AnalySIS Professional software (Soft Imaging Systems, Germany). Images were compiled using AnalySIS LS Professional software and Adobe Photoshop CS (Adobe Systems, San Jose, CA, USA).

Statistical analysis

Data are expressed as mean of cilium length ± SE. Cilium length changes were analysed using a one-way Analysis of Variance (ANOVA) with Tukey's *post hoc* test using GraphPad Prism 5.0 (GraphPad Software, San Diego, CA, USA) for inter-group comparisons.

Scanning electron microscopy (SEM)

UUO was induced as described above for a period of 10 days ($n = 2$) and uninjured mice were used as controls ($n = 2$). Mice were perfusion fixed with 2.5% phosphate-buffered glutaraldehyde. Kidneys were removed and fixed overnight in cacodylate buffer containing 2.5% glutaraldehyde, cryoprotected in 70% ethanol, freeze fractured using liquid nitrogen, rehydrated, postfixed in 1% osmium tetroxide in cacodylate buffer, washed in distilled H_2O, dehydrated through graded ethanol concentrations, washed three times in 100% ethanol and critical point dried in a Balzers CPD030 critical point dryer (Bal-Tec, Liechtenstein) with carbon dioxide gas as the transition fluid. Kidney fragments were mounted on aluminium stubs with the fractured surface facing upwards, coated with gold using a Balzers SCD005 sputter coater (Bal-Tec) and viewed using a Hitachi S570 (Hitachi, Tokyo, Japan) scanning electron microscope at Monash Micro-Imaging.

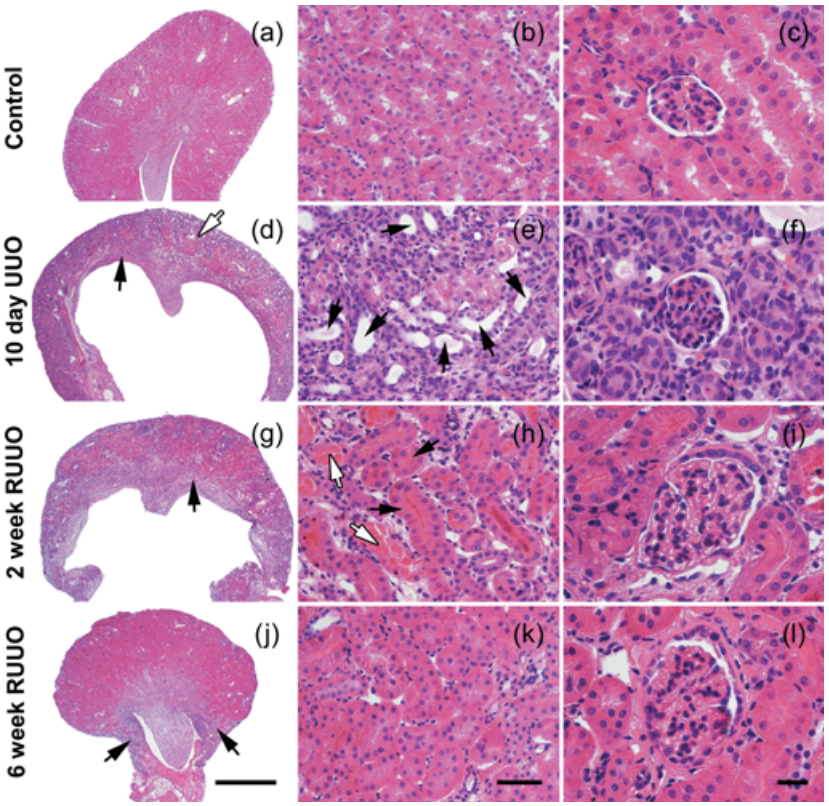

Fig. 2 The histology of UUO and repair following R-UUO. Examples of control kidney (a–c), 10 days of UUO (d–f) 2 weeks of R-UUO (g–i) and 6 weeks of R-UUO (j–l) are shown. In comparison with control kidney (a–c), 10-day UUO kidneys exhibit an ablation of the outer renal medulla (d, arrow) and significant thinning of the renal cortex (d, open arrow). This is accompanied by the appearance of dilated tubules and ducts lined by cells with a flattened morphology (e, arrows). Glomerular architecture was not grossly altered after 10 days of UUO (f). After 2 weeks of R-UUO, kidneys show a partial restoration of the renal medulla (g, arrow), the reappearance of differentiated epithelial cells that stain vividly pink with eosin in non-dilated tubules (h, arrows) and resolving tubular casts (h, open arrows). Six weeks of R-UUO results in a marked restoration of renal architecture (j,k); however, regions of remodelling are still evident (j, arrows). Glomeruli at 2 weeks (i) and 6 weeks (l) after R-UUO show hypertrophy. Scale bars: (j) 1000 μm, (a,d,g) the same magnification; (k) 50 μm, (b,e,h) the same magnification; (l) 20 μm, (c,f,i) the same magnification.

Results

The histology of UUO and R-UUO

The extent of renal injury in mice after UUO and R-UUO was determined by haematoxylin and eosin staining as shown in Fig. 2. The injury and repair processes following UUO and R-UUO have been documented in detail previously (Cochrane et al. 2005). Points to note in the context of the current study are that, compared with uninjured control samples (Fig. 2a–c), 10 days of UUO causes dilation of tubules and collecting ducts and loss of differentiated epithelial cells that stain vividly pink with eosin (Fig. 2d–f). There is widespread reversal of changes to the epithelial layer following 2 weeks of R-UUO (Fig. 2g–i) and near normal renal morphology after 6 weeks of R-UUO (Fig. 2j–l). Kidneys were generally smaller after 6 weeks of R-UUO, suggesting some nephron loss (Fig. 2j).

Renal cilia during UUO and R-UUO

Renal cilia were immunostained with anti-acetylated α-tubulin to investigate their distribution and dimensions during UUO and R-UUO (Fig. 3). This antibody detected cilia in the aquaporin-1-positive proximal tubule (Fig. 3a–d), the aquaporin-1-negative distal tubule and collecting duct (Fig. 3e–h), and on parietal epithelium of Bowman's capsule (Fig. 3i–l). Quantification of cilium length determined a significant increase in cilium length following 10 days of UUO in the proximal tubule (from 2.9 to 5.4 μm), distal tubule/collecting duct (from 3.0 to 6.7 μm) and on the parietal epithelium (from 2.8 to 5.3 μm) (Fig. 4a–c). Two weeks of R-UUO resulted in a significant regression of cilium length in the proximal tubule (from 5.4 to 3.6 μm) (Fig. 3a) and distal tubule/collecting duct (from 6.7 to 3.5 μm) (Fig. 3b). Six weeks of R-UUO resulted in further cilium length regression, including a statistically significant reduction in the length of cilia on the parietal epithelium when compared to 10 days of UUO (from 5.3 to 2.8 μm) (Fig. 4c).

Scanning electron microscopy of renal cilia in UUO

SEM of freeze fractured kidneys was used to observe renal cilia in 10-day UUO and control unobstructed kidneys (Fig. 5). The distal tubule (Fig. 5a,b) was identified by the characteristic cell morphology and taller microvilli at cell–cell junctions, and the collecting duct (Fig. 5c,d) by the presence of intercalated cells (Brenner & Rector, 1991). As the renal cilium is largely obscured by a brush border in the proximal tubule, the distal tubule and collecting duct provided the best opportunity to compare renal cilia in control and UUO material. Compared with control kidneys (Fig. 5a,c), there was an obvious lengthening of existing

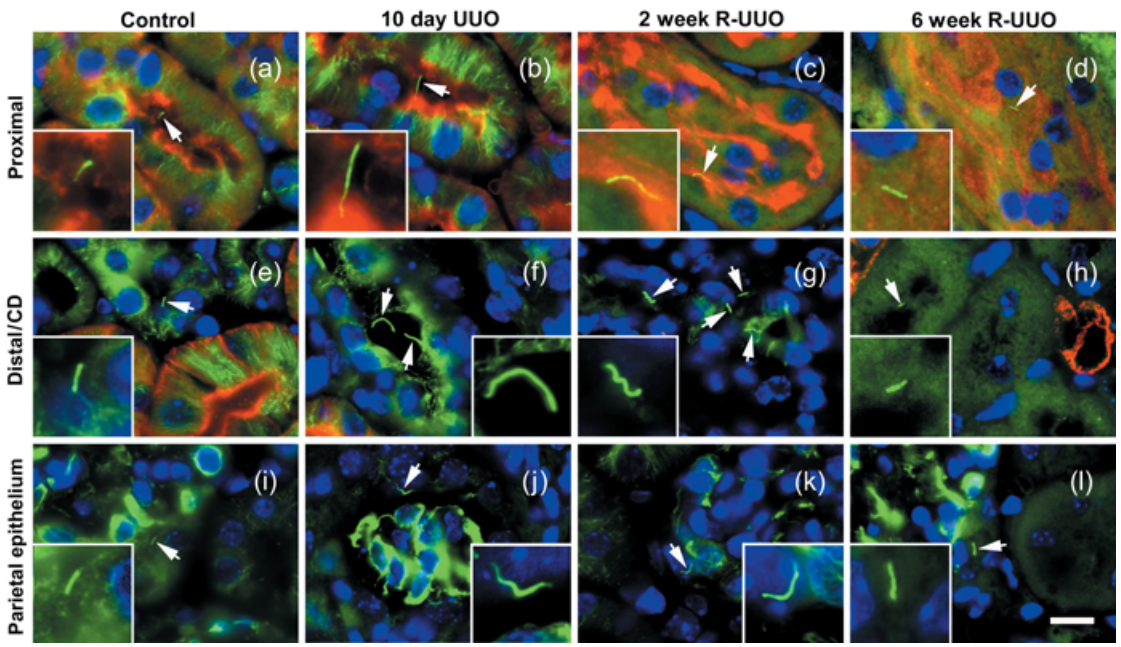

Fig. 3 Renal cilia during UUO and R-UUO. Renal cilia labelled with anti-acetylated α-tubulin (green, arrows & insets) are shown in the aquaporin-1-positive (red) proximal tubule (a–d), the distal tubule and collecting duct (e–f) and the parietal epithelium of Bowman's capsule (i–l). Nuclei are stained with DAPI (a–l). Renal cilia were approximately 3 mm long in sham operated control kidneys (a,e,i) and become dramatically longer after 10 days of UUO (b,f,j). A regression of this cilium lengthening was observed after 2 weeks (c,g,k) and 6 weeks of R-UUO (d,h,l). Scale bar: (l) 10 μm, (a–k) the same magnification. Insets showing detail of cilia in (a–l) are magnified an additional ×3.

cilia on epithelial cells in the distal tubule (Fig. 5b) and collecting duct (Fig. 5d) after UUO. The single cilium per cell arrangement that is typical of renal cilia is maintained after UUO injury (Fig. 5b,d).

Discussion

In this study we show that 10 days of UUO injury causes a dramatic increase in renal cilium length throughout the nephron and collecting duct of the affected kidney. Findings include the first report of cilium lengthening on the parietal epithelial layer (Bowman's capsule) of the glomerulus in response to injury. We previously demonstrated that 8 days of UUO caused cilium lengthening in the distal tubule and collecting duct, but no statistically significant change in cilium length was detected in the proximal tubule (Verghese et al. 2008). After the 10 days of UUO used in the present study, the kidney was on the brink of irreversible fibrotic injury (Cochrane et al. 2005) and this greater degree of injury also resulted in the lengthening of cilia in the proximal tubule. This apparent delay in cilium lengthening in the proximal tubule may due to the progression of tubular damage in UUO which primarily affects the collecting duct and distal tubule early in the course of injury (Cachat et al. 2003; Kida & Sato, 2007). However, distal tubule and collecting duct cilium lengthening in the absence of proximal tubule cilium lengthening has also been observed in transplanted human kidneys suffering rejection injury (manuscript in preparation). These results suggest that the proximal tubule is somewhat resistant to cilium lengthening when compared with the distal tubule and collecting duct. We have also documented the normalization of renal cilium length during the process of renal repair that occurs following the reversal of UUO. This normalization process largely takes place in the 2 weeks following reversal, but may take longer in Bowman's capsule. The 2-week time point is characterized by marked reepithelialization and a significant reduction in infiltrating inflammatory cells (Cochrane et al. 2005).

The degree of cilium lengthening we have documented by standard immunofluorescence microscopy probably represents a conservative estimate, due to that fact that longer cilia are less likely to be captured in a single plane of focus. However, this method does allow many examples of cilia to be collected relatively rapidly from defined segments of the nephron. We also note that the estimate of proximal tubule cilium length in uninjured kidney in the current study is less than in one of our previous studies (approximately 3 μm as opposed 4 μm) (Verghese et al. 2008). We attribute this difference to the citrate buffer antigen retrieval used in the current study providing better visualization of smaller cilia in the intact proximal tubule brush border than the proteinase K previously used for quantification.

SEM confirms the cilium length increases observed by immunofluorescence and also allows the number of cilia

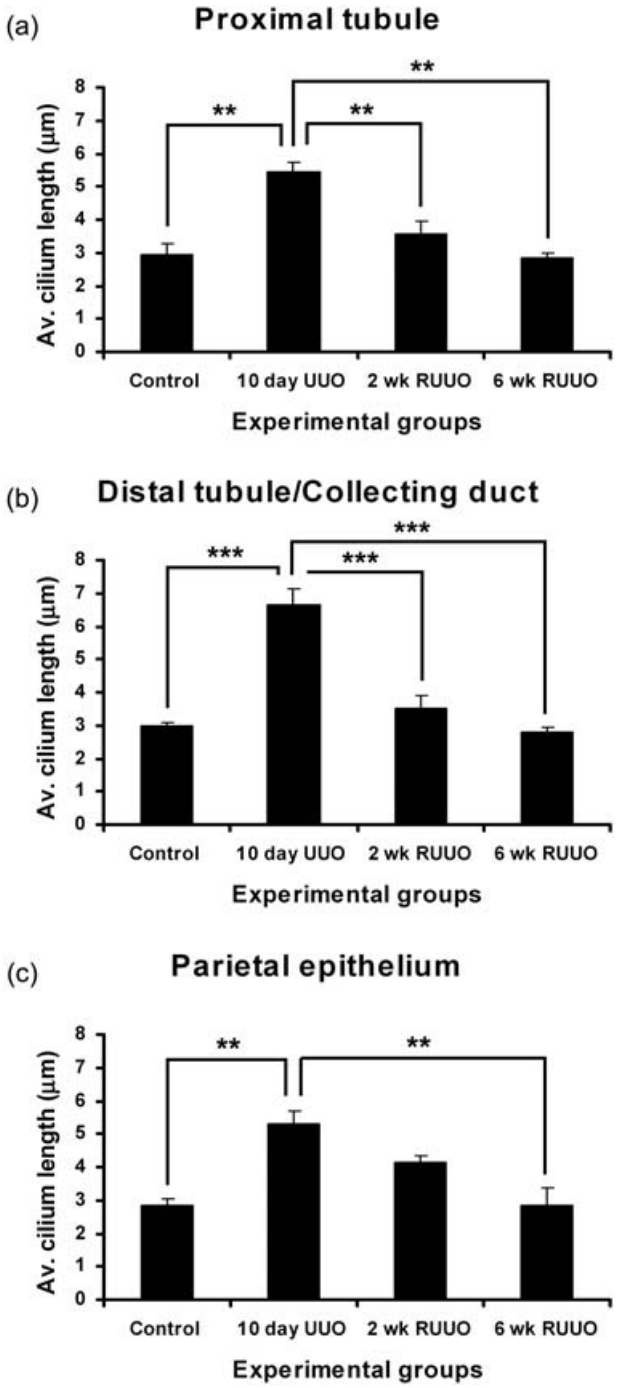

Fig. 4 Quantification of renal cilium length during UUO and R-UUO. Mean of average cilium length for the proximal tubule (a), the distal tubule (b) and the parietal epithelium of Bowman's capsule (c) is shown for control, 10-day UUO, 2-week R-UUO and 6-week R-UUO. $^{**}P < 0.01$, $^{***}P < 0.001$. Average cilium length was calculated from 20 cilia per segment for each mouse. Bars show standard error, $n = 3$ for all time points.

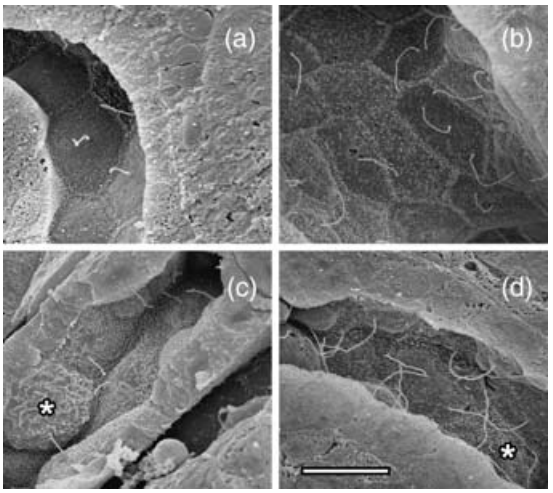

Fig. 5 Scanning electron microscopy of renal cilium lengthening after UUO. Renal cilia were visualized in the distal tubule (a,b) and the collecting duct (c,d). Normal-length cilia were observed in control uninjured distal tubule (a) and collecting duct (c). After 10 days of UUO, much longer cilia were present in distal tubule (b) and the collecting duct (d). The single cilium per cell arrangement seen in uninjured kidney (a,c) is maintained following injury (b,d). Intercalated cells in the collecting duct are marked with an asterisk (*) in (c,d). Scale bar in (d) = 7.5 μm, and (a–c) are at the same magnification.

per cell to be assessed. Although each epithelial cell in the kidney typically has only one renal cilium, multiple cilia per cell have been described in acute renal injury (Jones, 1982) and are more common in the Oak Ridge polycystic kidney mouse (Brown & Murcia, 2003). Scanning electron microscopy indicates that multiple cilia are not common after 10 days of UUO. Nearly all cells observed in injured kidney samples had the single cilium per cell arrangement that is characteristic of the uninjured epithelial layer. We conclude that increased cilium length following injury is due to the extension of existing cilia, rather than the emergence of an additional population of longer cilia.

The observed lengthening of renal cilia during injury raises questions as to the mechanisms that control cilium length in the kidney. The general nature of cilium lengthening suggests factors that affect the entire nephron and collecting duct system during UUO injury. Although the effect of 10 days of UUO on the architecture of the glomerulus is not dramatic, UUO has previously been demonstrated to cause gene transcription, protein expression and phenotypic changes in the renal epithelial layer that extend back along the nephron as far as Bowman's capsule (Diamond et al. 1995; Diamond et al. 1998; Feng et al. 2005). Candidate factors that may influence cilium length during UUO include the inflammatory environment of the injured kidney (Cochrane et al. 2005), cellular stretch responses caused by urinary backpressure (Diamond et al. 1998; Ricardo et al. 2000) and injury-associated reductions in glomerular filtration (Ito et al. 2004).

Although the underlying cause of this phenomenon has yet to be identified, the increase and subsequent regression of cilium length during injury appears to be a previously unappreciated indicator of renal injury and repair. With

further investigation and characterization, changes in renal cilium length may offer valuable insights into the severity, progression and recovery of renal disease in human patients. Moreover, the lengthening of renal cilia is likely to influence epithelial differentiation in the renal tubule and duct during injury and repair. There is a strong body of evidence supporting the notion that flow-mediated deflection of the renal cilium promotes the maintenance of epithelial differentiation in the renal tubule and duct. Studies also suggest that the sensitivity of the renal cilium to flow is positively correlated to its length (Schwartz et al. 1997; Liu et al. 2005; Resnick & Hopfer, 2007). We have proposed that the lengthening of renal cilia following injury is a compensatory response that increases the sensory sensitivity of this organelle and promotes epithelial differentiation (Verghese et al. 2008). Increased cilium sensitivity may balance the propensity for epithelial dedifferentiation that exists following injury and facilitate the process of epithelial redifferentiation that is required for repair (Bonventre, 2003). Such a mechanism is potentially important in UUO and other forms of renal injury where mechanical input to the cilium is reduced by decreased urine flow. The regression of cilium length we observe following R-UUO coincides with the widespread re-establishment of a differentiated epithelial layer and may indicate a reduced requirement for cilium-mediated epithelial redifferentiation.

In summary, we have described a generalized increase and regression of renal cilium length during UUO injury and repair that may be an important indicator of epithelial injury, and a mediator of repair. Further investigation will be required to determine the factors that trigger this increase in cilium length and to fully appreciate its implications for cilium-based signalling during epithelial repair. A better understanding of the renal cilium during epithelial damage and repair may provide new avenues for monitoring and altering the course of renal injury and disease in a clinical setting.

Acknowledgements

J.A.D. is funded by the National Health and Medical Research Council of Australia and has received funding from Kidney Health Australia. S.D.R. is a recipient of the Kidney Health Australia Bootle bequest. The authors acknowledge the assistance of the staff at Monash MicroImaging, Ian Boundy for histology, Anita Cochrane for providing mouse kidney samples and the members of the MISCL Renal Laboratory for their help and advice.

References

Bonventre JV (2003) Dedifferentiation and proliferation of surviving epithelial cells in acute renal failure. *J Am Soc Nephrol* **14** (Suppl. 1), S55–61.

Brenner BM, Rector FC (1991) *The Kidney*. W. B. Saunders Company, Philadelphia.

Brown NE, Murcia NS (2003) Delayed cystogenesis and increased ciliogenesis associated with the re-expression of polaris in Tg737 mutant mice. *Kidney Int* **63**, 1220–1229.

Bulger RE, Siegel FL, Pendergrass R (1974) Scanning and transmission electron microscopy of the rat kidney. *Am J Anat* **139**, 483–501.

Cachat F, Lange-Sperandio B, Chang AY, et al. (2003) Ureteral obstruction in neonatal mice elicits segment-specific tubular cell responses leading to nephron loss. *Kidney Int* **63**, 564–575.

Cochrane AL, Kett MM, Samuel CS, et al. (2005) Renal structural and functional repair in a mouse model of reversal of ureteral obstruction. *J Am Soc Nephrol* **16**, 3623–3630.

Diamond JR, Kees-Folts D, Ricardo SD, Pruznak A, Eufemio M (1995) Early and persistent up-regulated expression of renal cortical osteopontin in experimental hydronephrosis. *Am J Pathol* **146**, 1455–1466.

Diamond JR, Kreisberg R, Evans R, Nguyen TA, Ricardo SD (1998) Regulation of proximal tubular osteopontin in experimental hydronephrosis in the rat. *Kidney Int* **54**, 1501–1509.

Feng D, Imasawa T, Nagano T, et al. (2005) Citrullination preferentially proceeds in glomerular Bowman's capsule and increases in obstructive nephropathy. *Kidney Int* **68**, 84–95.

Ito K, Chen J, El Chaar M, et al. (2004) Renal damage progresses despite improvement of renal function after relief of unilateral ureteral obstruction in adult rats. *Am J Physiol Renal Physiol* **287**, F1283–F1293.

Jones DB (1982) Ultrastructure of human acute renal failure. *Lab Invest* **46**, 254–264.

Kida Y, Sato T (2007) Tubular changes in obstructed kidney of adult mice evaluated using immunohistochemistry for segment-specific marker. *Histol Histopathol* **22**, 291–303.

Liu W, Murcia NS, Duan Y, et al. (2005) Mechanoregulation of intracellular Ca^{2+} concentration is attenuated in collecting duct of monocilium-impaired orpk mice. *Am J Physiol Renal Physiol* **289**, F978–88.

Liu Y (2004) Epithelial to mesenchymal transition in renal fibrogenesis: pathologic significance, molecular mechanism, and therapeutic intervention. *J Am Soc Nephrol* **15**, 1–12.

Nauli SM, Alenghat FJ, Luo Y, et al. (2003) Polycystins 1 and 2 mediate mechanosensation in the primary cilium of kidney cells. *Nat Genet* **33**, 129–137.

Pazour GJ, Dickert BL, Vucica Y, et al. (2000) Chlamydomonas IFT88 and its mouse homologue, polycystic kidney disease gene tg737, are required for assembly of cilia and flagella. *J Cell Biol* **151**, 709–718.

Praetorius HA, Spring KR (2003a) Removal of the MDCK cell primary cilium abolishes flow sensing. *J Membr Biol* **191**, 69–76.

Praetorius HA, Spring KR (2003b) The renal cell primary cilium functions as a flow sensor. *Curr Opin Nephrol Hypertens* **12**, 517–520.

Praetorius HA, Frokiaer J, Nielsen S, Spring KR (2003) Bending the primary cilium opens Ca^{2+}-sensitive intermediate-conductance K^+ channels in MDCK cells. *J Membr Biol* **191**, 193–200.

Resnick A, Hopfer U (2007) Force-response considerations in ciliary mechanosensation. *Biophys J* **93**, 1380–1390.

Ricardo SD, Franzoni DF, Roesener CD, Crisman JM, Diamond JR (2000) Angiotensinogen and AT(1) antisense inhibition of osteopontin translation in rat proximal tubular cells. *Am J Physiol Renal Physiol* **278**, F708–16.

Schwartz EA, Leonard ML, Bizios R, Bowser SS (1997) Analysis and modeling of the primary cilium bending response to fluid shear. *Am J Physiol* **272**, F132–8.

Verghese E, Weidenfeld R, Bertram JF, Ricardo SD, Deane JA (2008) Renal cilia display length alterations following tubular

injury and are present early in epithelial repair. *Nephrol Dial Transplant* **23**, 834–841.

Webber WA, Lee J (1974) The ciliary pattern of the parietal layer of Bowman's capsule. *Anat Rec* **180**, 449–455.

Webber WA, Lee J (1975) Fine structure of mammalian renal cilia. *Anat Rec* **182**, 339–343.

Wheatley DN, Wang AM, Strugnell GE (1996) Expression of primary cilia in mammalian cells. *Cell Biol Int* **20**, 73–81.

Wilson PD (2004) Polycystic kidney disease. *N Engl J Med* **350**, 151–164.

Yoder BK, Mulroy S, Eustace H, Boucher C, Sandford R (2006) Molecular pathogenesis of autosomal dominant polycystic kidney disease. *Expert Rev Mol Med* **8**, 1–22.

Yoder BK, Tousson A, Millican L, et al. (2002) Polaris, a protein disrupted in orpk mutant mice, is required for assembly of renal cilium. *Am J Physiol Renal Physiol* **282**, F541–52.